Ultrasonic investigation of the evaporation dynamics of subnanoliter droplets

Quy Raven Luong, Andreas Hefele, Alexander Reiner, Andreas Hörner, Achim Wixforth

Angaben zur Veröffentlichung / Publication details:

Luong, Quy Raven, Andreas Hefele, Alexander Reiner, Andreas Hörner, and Achim Wixforth. 2021. "Ultrasonic investigation of the evaporation dynamics of subnanoliter droplets." Journal of Applied Physics 130 (22): 224702. https://doi.org/10.1063/5.0072146.

Journal of Applied Physics

Ultrasonic investigation of the evaporation dynamics of subnanoliter droplets

Cite as: J. Appl. Phys. **130**, 224702 (2021); https://doi.org/10.1063/5.0072146
Submitted: 20 September 2021 • Accepted: 21 October 2021 • Published Online: 08 December 2021

Quy Raven Luong, Andreas Hefele, Alexander Reiner, et al.

Journal of Applied Physics ARTICLE scitation.org/journal/jap

Ultrasonic investigation of the evaporation dynamics of subnanoliter droplets

Cite as: J. Appl. Phys. **130**, 224702 (2021); doi: 10.1063/5.0072146
Submitted: 20 September 2021 · Accepted: 21 October 2021 ·
Published Online: 8 December 2021

View Online Export Citation CrossMark

Quy Raven Luong,[1] Andreas Hefele,[1] Alexander Reiner,[1] Andreas Hörner,[1] and Achim Wixforth[1,2,3,a)]

AFFILIATIONS

[1]Experimental Physics 1, University of Augsburg, 86159 Augsburg, Germany
[2]Augsburg Center for Innovative Technologies ACIT, 86159 Augsburg, Germany
[3]Center for NanoScience, CeNS, 80331 Munich, Germany

[a)]**Author to whom correspondence should be addressed:** achim.wixforth@physik.uni-augsburg.de

ABSTRACT

With the development of ink jet printers or spotters for biological applications, the control size and homogeneity of small fluids as well as their successful deposition on various substrates has gained significant importance. We study the impingement process of such small droplets onto a solid substrate and investigate their evaporation and drying process by means of surface acoustic wave (SAW) transmission experiments. We observe a strong fluid-SAW interaction resulting in an attenuation which toward the end of the evaporation and drying process exhibits characteristic oscillations being related to temperature, SAW amplitude, and fluid properties such as viscosity and wetting angle. It is found that oscillations can only be seen in pinned, very flat droplets, while the pinning can be roughly controlled via the SAW amplitude. The frequency of those characteristic oscillations is superlinear with respect to temperature, rather proportional to the evaporation rate and can change drastically depending on the liquid used. In our experiments, isopropanol, ethanol, and water with various glycerol concentrations were loaded onto the SAW delay line. Based on the experimental results, simulations using the finite element method were performed. We find that a standing wave pattern within the droplet is responsible for the transmission oscillations. These findings might lead to new methods, e.g., sensory systems, being able to examine droplets according to their physical or chemical properties.

I. INTRODUCTION

Since the development of application involving combustion, spray cooling, ink jet printing, and others, the physics of evaporation has become of great interest. Numerous studies have examined the dependence of droplet evaporation on the droplet properties,[1,2] substrate properties,[3,4] and environmental influences,[5,6] often focusing on the dynamics of the contact line during evaporation using optical experiments. Here, the evaporation process is investigated by sampling the droplet with surface acoustic waves.

Surface acoustic waves have become an essential part of many applications as well and are widely employed in a variety of devices for telecommunication,[7,8] radio frequency signal processing,[9] biochemical sensory systems,[10] microfluidics,[11,12] and more. The basic idea behind these devices is that the acoustic energy is mainly bound to the surface of a piezoelectric substrate on which they propagate along and can easily be manipulated by changes on the surface, e.g., by mass loading. Specifically, in the field of microfluidics, SAW is often employed on the so-called lab-on-a-chip, where they can effectively be used for various tasks like inducing an acoustic streaming in small amounts of fluids. This can already be done at low SAW amplitudes and allow an easy way for acoustic mixing. At higher amplitudes, the acoustic streaming is even able to deform an entire droplet and can lead to a SAW driven displacement, which has become the basis for SAW driven actuation. SAW can also be used for droplet heating or, if its power is high enough, for jetting and atomization.[13]

In the present work, an evaporating nanoliter droplet of water is monitored via surface acoustic waves by placing the drop on a SAW delay line and measuring the transmitted SAW signal. At first glance, evaporation of a liquid seems to be just an everyday process and maybe even trivial. But in microfluidics, evaporation can oftentimes be an unwanted process and become quite a big issue when working with very small amounts of fluids in open air, leading to a quick dry out of the fluid reservoir and failure of the device.[14]

Efforts are therefore usually made to prevent or at least minimize evaporation and are frequently done by enclosing the reservoir in mineral oil[15,16] to block any open air interface. On the other hand, evaporation and/or drying of small spotted droplets might also be a deliberate process, for instance, the preparation of microarrays.[17] In this work, however, the evaporation of the nanoliter droplet spotted on the SAW delay line leads to a very interesting behavior in the transmitted signal. Characteristic oscillations are observed in the signal toward the end of the evaporation process. The exact cause of these oscillations, though, is largely unknown and to date no publications explaining or even reporting these oscillations have been found so far. To analyze this observation and find an explanation, various parameters that can potentially influence these oscillations were examined. It is assumed that the oscillations strongly depend on the SAW interaction as well as properties of the fluid and therefore could become the basis for future applications like a new sensory system to characterize any liquid droplet by its physical properties, chemical composition, or surrounding environment.

II. EXPERIMENTAL SETUP

Surface acoustic waves are generated and detected using a delay line configuration, consisting of two opposing straight interdigital transducers (IDTs) on a $LiNbO_3$ substrate as shown in Fig. 1.

Each of those IDTs consists of two comb-like electrodes and induces a deformation of the substrate beneath due to the inverse piezoelectric effect when a voltage is applied. If the voltage is harmonic, a periodic deformation is induced to the substrate and as a result leads to the launch of the SAW with the same frequency, the wavelength being determined by the periodicity of the IDT. For $LiNbO_3$ and the chosen crystal cut (128°Y-Cut), the generated SAW is of Rayleigh type,[18] which has longitudinal as well as transverse vibrations along its propagation, leading the lattice points close to the surface to move in an elliptical fashion. Similarly, the whole SAW generation process works also in the opposite direction, which is known as the inverse piezoelectric effect and is used at the other IDT to detect the generated, attenuated SAW. The incoming SAW is then converted back to an electrical signal. In our case, the resonance frequency of the IDTs was at $f_{SAW} = 158$ MHz.

A water droplet of about $V = 0,8$ nl is dispensed by a GeSiM nanoliter dispenser onto the delay line, causing an attenuation of the transmitted signal because the SAW is partially leaked into the droplet. Eventually, the droplet evaporates completely and the attenuation disappears. To measure the transmitted signal as a function of time, a spectrum analyzer was used in zero span mode. Such a transmitted signal is illustrated in Fig. 2 as an example. After dispensing the fluid, the amplitude of the transmitted signal is significantly lowered as one would expect due to the impinged droplet in the SAW path. However, the most interesting and unexpected behavior can be seen right before the magnitude of the transmitted signal goes back up when the droplet is about to completely evaporate. Characteristic oscillations forming an up-chirp can be observed toward the end. A finite element method simulation based on the results as being discussed later was carried out, which provides a good explanation for the observed oscillations.

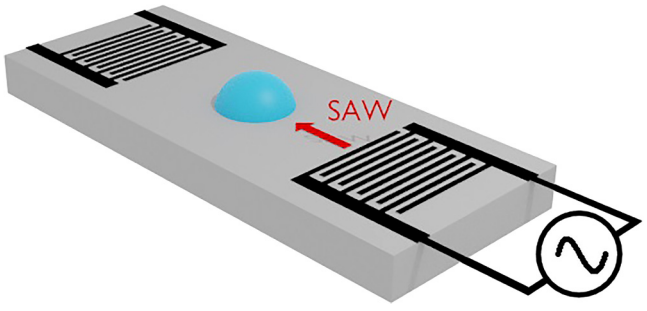

FIG. 1. Experimental setup for the sampling of droplets with surface acoustic waves.

III. RESULTS AND DISCUSSION

The current presumption is that the characteristic oscillations arise due to the formation of standing waves inside the droplet by the SAW. In general, SAW-induced standing waves in nanoliter droplets for different SAW frequencies and droplet sizes have already been studied by Shilton *et al.*[19] The characteristic oscillations, however, have not yet been reported. To unravel the cause of this phenomenon, various parameters like SAW amplitude, frequency, and temperature were varied; their influence on those oscillations has been studied.

In general, these oscillations were found to only arise in evaporating droplets with pinned contact line, meaning that the initial contact radius remains constant, while the contact angle decreases over time. In droplets evaporating in constant contact angle mode, such oscillations could not be distinctively observed. The two

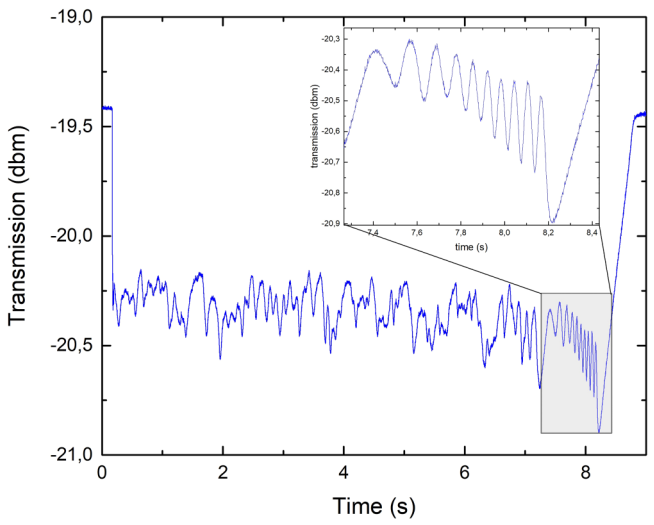

FIG. 2. Measurement of the time dependent transmitted SAW signal being attenuated by the nanoliter water droplet in the SAW path. Right before the droplet completely evaporates and the signal recovers to its initial value, characteristic oscillations can be observed.

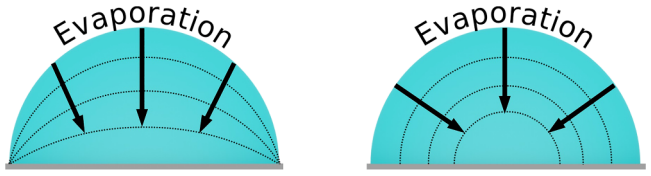

FIG. 3. Demonstration of constant contact radius (left) and constant contact angle (right) evaporation mode. The black dashed line represents the free surface decreasing over time.

evaporation modes are demonstrated in Fig. 3. Hence, if not stated otherwise, the droplets are considered to evaporate in constant contact radius mode. A video of a real-time measurement is included in the supplementary material for visualization.

A. Influence of SAW amplitude

The transmitted signal was analyzed for various SAW amplitudes. Measurements done at the input powers of $P_{SAW} = -12$ dbm and $P_{SAW} = +15$ dbm are exemplary shown in Fig. 4. The oscillation can only be distinctively measured at low enough SAW amplitudes as the drop contact line is being pinned to the substrate, which was observed using a microscope. The droplet pinning, however, becomes overwhelmed by an increased SAW amplitude causing the droplet to deform and decreasing its contact area near the end of the evaporation process. In this case, such oscillations become more difficult to observe or even cannot be seen at all like in Fig. 4, bottom. Therefore, in order to reproduce those oscillations, a low SAW amplitude is recommended.

Generally, the attenuation of the transmitted signal mainly depends on the contact area of the droplet rather than the droplet mass and remains relatively constant over time as long as the contact area stays constant as well.

B. Influence of temperature

The oscillation frequency was measured at various temperatures as shown in Fig. 5. The cooling of the SAW delay line was done thermoelectrically using a Peltier element. It is found that the frequency is superlinear with respect to temperature and most interestingly, the characteristic oscillation can only be observed above the dew point, implicating that the evaporation process must be essential for them to occur. This can easily be proven by carrying out the exact same experiment at different experimental conditions and a lower dew point (roughly 3 °C). It is shown that the characteristic oscillation frequencies are generally higher compared to the frequencies for higher dew point and cannot be observed again once the dew point is reached. Therefore, it is safe to assume that the oscillation frequency is proportional to the evaporation rate and less dependent on temperature. However, temperature does also change physical properties like viscosity or speed of sound, which surely affect those oscillations. In this case, a mean evaporation rate is being approximated and represented by inverting the lifetime τ of the droplet so that the proportionality is described by

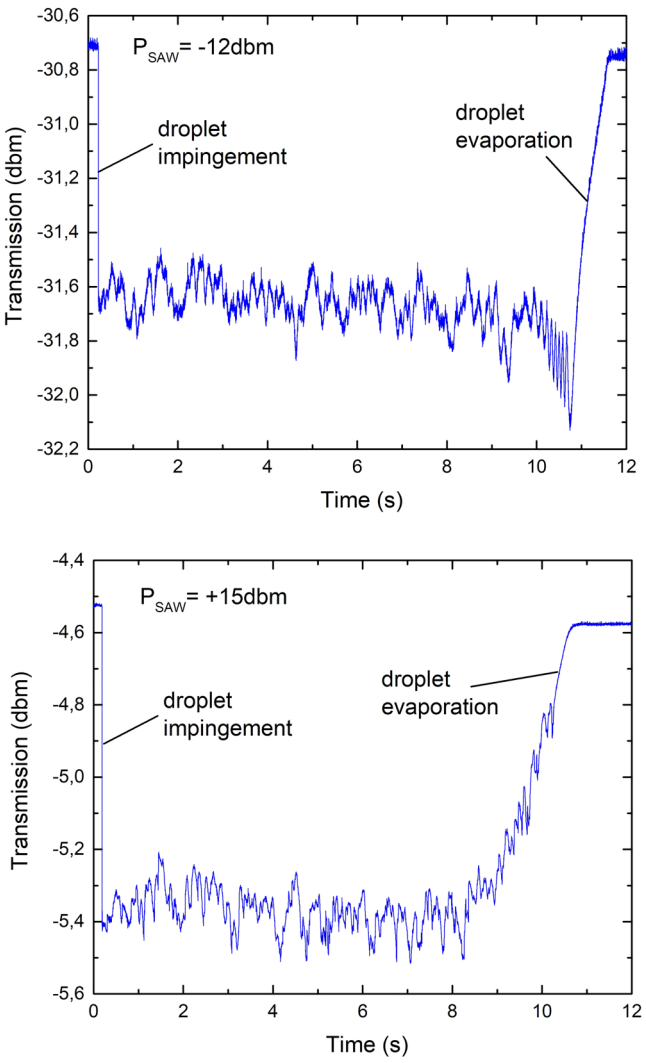

FIG. 4. Measured transmitted SAW signal for different input powers (top: $P_{SAW} = -12$ dbm; bottom: $P_{SAW} = +15$ dbm). The oscillations can be best observed at lower input powers. At higher input powers, the droplet becomes depinned from the substrate, causing the contact area to decrease during evaporation and making the oscillations difficult to observe.

$$f = \frac{\alpha}{\tau}, \tag{1}$$

with α being a dimensionless constant value. For the dew points at $T = 12$, 5, and 3 °C, α was determined to be $\alpha = 120$ and $\alpha = 106$, respectively. The small variation in the constant is due to small variations in the droplet sizes. In fact, differently sized droplets were also dispensed in the experiment, but had no effect on the frequency, keeping the contact area constant.

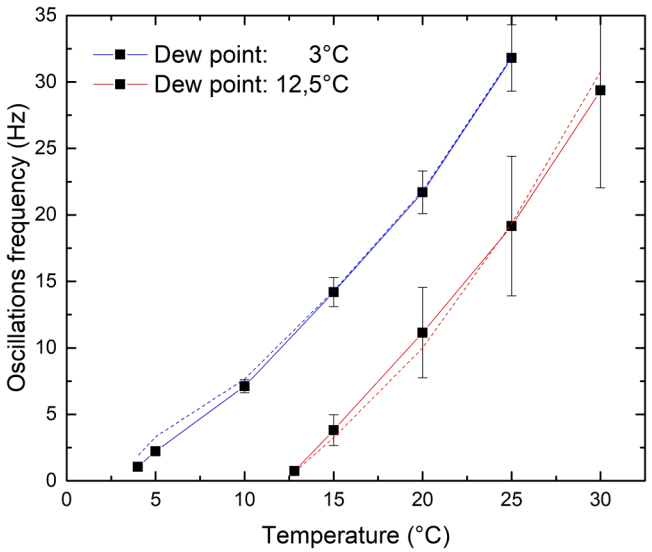

FIG. 5. Oscillation frequency shown by the solid lines/data points at various temperatures. The dashed lines represent the calculated frequency based on Eq. (1).

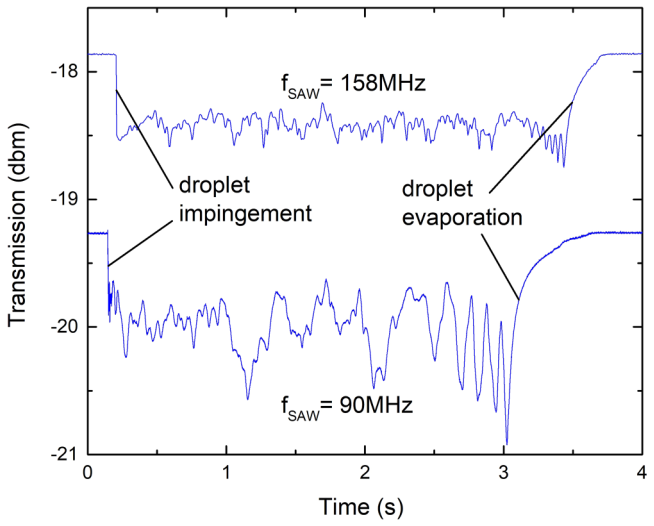

FIG. 6. SAW transmission signal measured for $f_{SAW} = 158$ MHz (upper curve) and $f_{SAW} = 90$ MHz (lower curve). The oscillation frequency was found at $f_{osc} = 23$ Hz and $f_{osc} = 9$ Hz, respectively.

For now, this leads to a first conclusion that the oscillations either must be a macroscopic vibration induced by the evaporation itself, or arise because of the droplet reaching certain phases allowing geometrical vibrational modes to be excited by the SAW.

C. Influence of SAW frequency

To further verify this conclusion, the transmission signal was measured for two different delay lines with resonance frequencies of $f_{SAW} = 158$ MHz and $f_{SAW} = 90$ MHz, respectively. The oscillation frequencies of both delay lines were then measured to be $f_{osc} = 23$ Hz and $f_{osc} = 9$ Hz, respectively (see Fig. 6). This indicates that the oscillations are not caused by any macroscopic vibrations due to the evaporation process or initial impact on the substrate, but rather by vibrational modes inside the droplet excited by the SAW.

The droplet itself can be described as a confined system, in which acoustic waves originating from the SAW can propagate and eventually form geometrically standing waves whenever the necessary resonance conditions are fulfilled. This, however, is only true if the droplet reaches a certain geometry as a result of the evaporation process, meaning that the observed characteristic oscillations are caused by alternating conditions for constructive and destructive interferences. Lower SAW frequencies or longer SAW wavelengths, while the evaporation rate remains the same, consequently mean that the droplet needs more time to reach the next geometric state in which standing waves can form and therefore causes a decrease in the oscillation frequency as well as in the number of oscillations since fewer wavelengths can fit in.

D. Influence of different fluids used

Isopropanol and ethanol instead of pure water have also been dispensed for comparison (see Fig. 7). The oscillation frequency was measured at $f_{SAW} = 158$ MHz to be $f_{osc} = 150$ Hz and $f_{osc} = 100$ Hz, respectively. It is higher for both alcohols than for water due to their much higher evaporation rate. It should be noted, however, that both alcohols are weakly bound to the substrate so that most of the time the signal recovers to its initial value even without the occurrence of the characteristic oscillations due to missing droplet pinning in contrast to the more step-like recovery for pinned droplets. Usually, the alcohol droplet evaporates in a constant contact angle mode, but sometimes switches to the constant contact area evaporation mode, most probably due to some residual contamination from previous droplets, forcing the pinning. Hence, to analyze this behavior further in the future, additional efforts have to be considered to enable the pinning for different liquids.

To study a possible influence of viscosity, water with various glycerol concentrations has been used (see Fig. 8) and the results are shown in Fig. 9. In this case, the oscillation frequency decreases for higher glycerol concentration as well as becoming a lot harder to reproduce, similar to the results for the alcohols. In contrast to the previous pure water, the droplet no longer completely evaporates, which is shown by the fact that the signal does not recover to its initial value (see Fig. 8). The main reason is the different evaporation rate for water and glycerol, causing water to be completely removed from the droplet while glycerol remains as a residue. At higher glycerol concentrations, the characteristic oscillation could not be observed, presumably because of the residue droplet having a constant volume and not reaching the geometric phases of interest.

IV. USING FEM SIMULATION TO SHOW THE TRANSITION OF FLUID TO PURE SAW DETECTED EIGENMODES IN A 2D DROPLET SLICE

Based on the results so far and to obtain a better understanding, a combined solid state and pressure acoustic FEM simulation

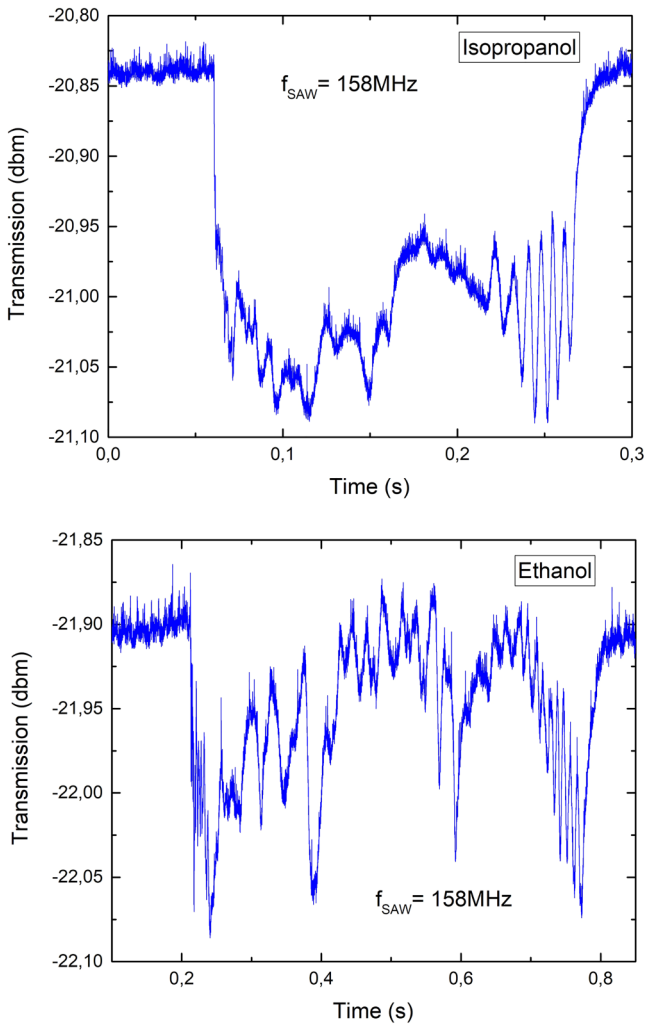

FIG. 7. Measured transmission after dispensing an isopropanol (top) and an ethanol (bottom) droplet for $f_{SAW} = 158$ MHz. The frequencies of the characteristic oscillations were $f_{osc} = 150$ Hz and $f_{osc} = 100$ Hz, respectively.

in the frequency domain was set up and carried out, using COMSOL Multiphysics. Looking at the schematic [Fig. 10, Multimedia view], the SAW is generated at the left side of the droplet and propagates linearly to the right, while interacting with the droplet, just like in the experiment. Every simulation step corresponds to a certain point in time and droplet height B with the height decreasing with time. The excerpts show a two-dimensional cross section of an elliptical droplet at two different times. At $t = t_1$, the center height of the droplet is $B_1 = 0.14\lambda_{SAW} = 0.5\lambda_{fluid}$ and roughly 6/7 of the droplet width are dominated by acoustic eigenmodes inside the fluid (methanol). The time $t = t_2$ corresponds to a droplet height of $B_2 = 0.07\lambda_{SAW} = 0.25\lambda_{fluid}$, at which the acoustic fluid eigenmodes in the droplet disappear.

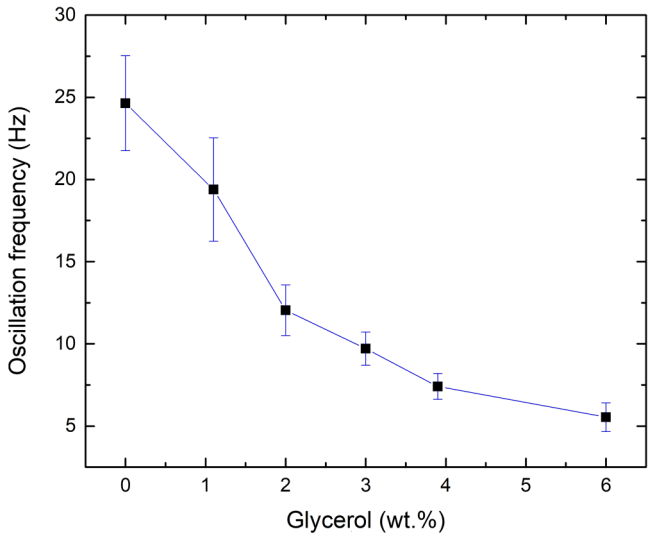

FIG. 8. Measured SAW transmission after dispensing a water droplet with a 2 wt. % glycerol concentration.

A. Analytical estimation of the chirped characteristic oscillations

For an analytical estimate of the chirped signal, the x-positions of the transition heights H to the left and right sides of the droplet center must be considered, because the fluid wavelength converts into the SAW wavelength at these positions and thin film considerations referring to the SAW wavelength become dominant.

If the wavelength of the fluid is smaller than the SAW wavelength, which is generally the case, the total number of standing waves inside the droplet in the x-direction decreases with decreasing droplet height. The oscillation signal that presumably shows constructive and destructive interference of the wave inside the shrinking droplet stops, when $H = B$ because of the fluid layer being too thin for standing waves to form inside.

To calculate the x-position x_i of the constant height H_i for any fluid i as a function of the central height B of the droplet, the characteristic function of an ellipse is considered,

$$(x/A)^2 + (y/B)^2 = 1. \tag{2}$$

Here, A is the fixed contact radius of the droplet. Solving for x_i and substituting y with $H_i =$ constant yields

$$x_i(B) = \sqrt{1 - (H_i/B)^2}A. \tag{3}$$

The constant H_i moves from the edge of the droplet to the center during the shrinking of B from B_1 to B_2 as shown in Fig. 10.

The behavior of the corresponding transmitted acoustical SAW signal P_i is specified to be sinusoidal. During the shrinking, the droplet area in which the fluid eigenmodes can form becomes smaller toward the center of the droplet, and thus the leaked SAW

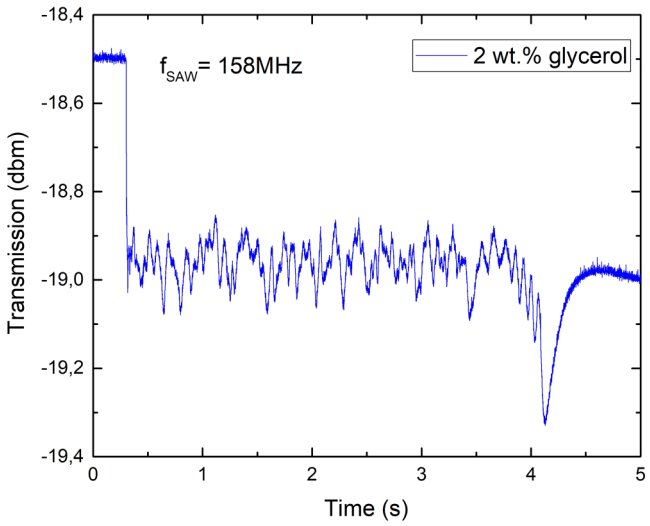

FIG. 9. Frequency of the charactersitic oscillations for various glycerol water concentration (wt. %).

is subject to alternating constructive and destructive interference conditions. As a result, the transmitted power oscillates as a function of time. With an assumed periodicity of the fluid wavelength, the time dependent sinusoidal behavior of the SAW passing the droplet can be described by

$$P_i(B) \propto \sin^2\left(\frac{2\pi}{\lambda_i} x_i(B)\right). \tag{4}$$

Substituting Eq. (3) in (4) yields

$$P_i(B) \propto \sin^2\left(\frac{2\pi}{\lambda_i}\sqrt{1-(H_i/B)^2}A\right). \tag{5}$$

Because the transition from the standing wave area inside the droplet to a thin fluid layer without a standing wave area is relatively smooth, the actual disappearance of the function at $B = H_i$ is also not step-like. An idea would be to introduce an additional Fermi function like step of the form $1/(\exp((H_i - B)/a) + 1)$ and multiply with Eq. (5), resulting in

$$P_i(B) \propto \frac{\sin^2\left(\frac{2\pi}{\lambda_i}\sqrt{1-(H_i/B)^2}A\right)}{\exp\frac{H_i-B}{a}+1}, \tag{6}$$

where a is a constant. However, since $P_i(B)$ is only valid for $B \geq H_i$, the step-function does not really apply.

As described before, the attenuation of the signal is mainly influenced by the contact area. Assuming that the droplet needs a minimum height to be able to absorb SAW at all, then there must be an effective area A_{eff} at that certain height, which remains constant during most of the lifetime of the droplet and rapidly decreases

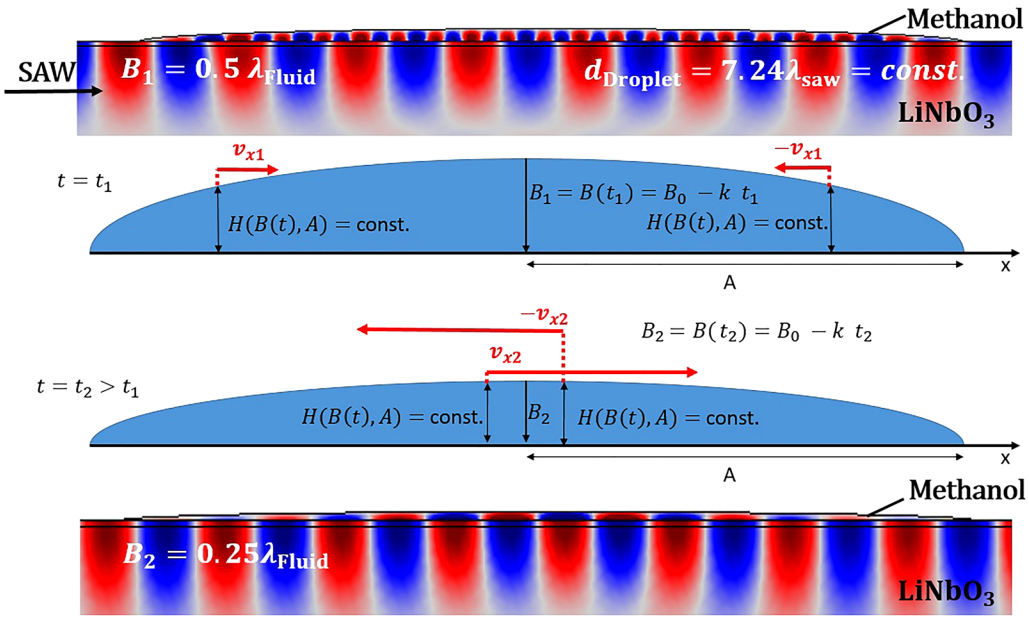

FIG. 10. Two excerpts of the simulation in the frequency domain, assuming a constant shrinking rate k of a droplet. The droplet base is pinned to the substrate. At $t = t_1$, the center height of the droplet is $B_1 = 0.5\lambda_{\text{fluid}}$ and, in the inner 6/7 of the drop width, acoustic eigenmodes (frequency: 180 MHz) can be clearly seen, the wavelength being determined by the fluid (methanol). The time $t = t_2$ corresponds to a droplet height of $B_2 = 0.25\lambda_{\text{fluid}}$, at which the fluid eigenmodes disappear and instead the modes become purely determined by the Rayleigh wave instead. Multimedia view: https://doi.org/10.1063/5.0072146.1.

shortly before complete evaporation, causing the overall step-like recovery and the change in amplitude of the characteristic oscillations. This can then be described by

$$P_i(B) = P_0 - P_{\mathrm{osc}}(B)\sin^2\left(\frac{2\pi}{\lambda_i}\sqrt{1-(H_i/B)^2}A\right) - IA_{\mathrm{eff}}(B), \tag{7}$$

with P_0 being the transmitted power without any attenuation, P_{osc} being the amplitude of characteristic oscillations, and I being the intensity of the absorbed SAW.

Since the simulation is simplified to a two-dimensional problem and the step behavior itself is not that interesting as being compared to the chirping of the signal, we omit this discussion at this point.

B. Numerical solutions

The power of the transmitted signal was calculated and is plotted as a function of the droplet height in Fig. 11 which shows the results of the simulation for different fluids (top) and SAW frequencies in water (bottom). All signals indeed show the expected chirp like signal. The already discussed point in time, where the eigenmodes of the droplet disappear, is also marked. These points were all identified at a height of $0.26\lambda_{\mathrm{fluid}}$. Therefore, it is most likely that the signals are—apart from offsets due to, e.g., viscosity related power dissipation—similar, if plotted as a function of the fluid wavelength.

Figure 12 shows the simulated transmitted SAW power and the analytically calculated signal based on Eq. (6) as functions of height for the methanol droplet. While the direct comparison does not show a very good match, relatively good agreement between the numerical solution and the analytical estimation can still be seen nevertheless.

To compare the simulation and the experiment, the relation between time and droplet height is of great importance because the simulation does not explicitly include any time dependence. Hence, the height was measured experimentally and found to decrease linearly with time, which is why the height was defined in the simulation like that as well. Exact height measurements, however, are very difficult and become actually impossible when the droplet becomes too small. Still, the negative linear relationship is typical for pinned droplet evaporation. Various studies on the evaporation process of droplets on substrates show that the contact angle decreases linearly with time.[20–22] Since the central height of a droplet can be

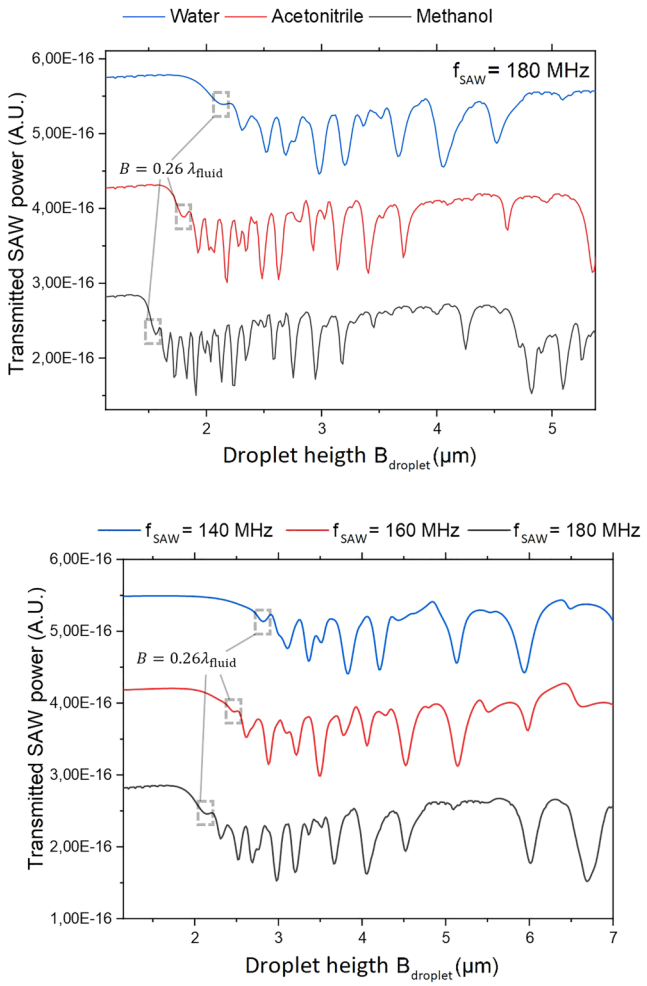

FIG. 11. Simulated transferred electrical SAW energy for different fluids (top) and SAW frequencies (bottom). The offset between the traces has been introduced for better visibility.

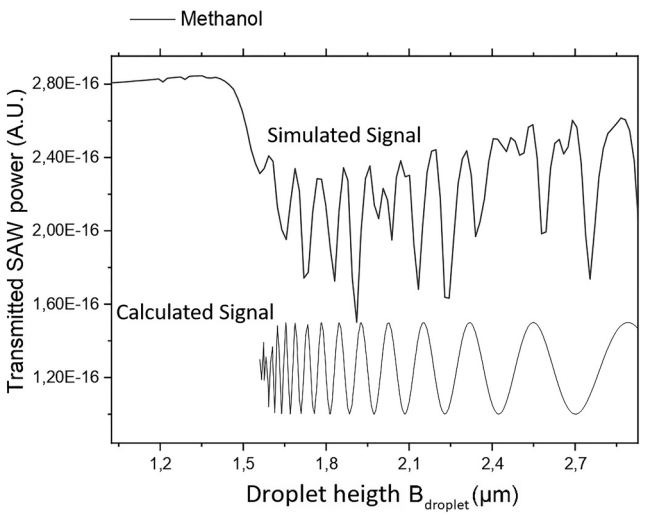

FIG. 12. Simulated transmitted SAW power compared to the analytically calculated signal of a 2D simulated methanol droplet slice. For the calculation, Eq. (6) is used with $H_i = 0.25\lambda_{\mathrm{fluid}}$, in the case of methanol $H_i = 1.5\,\mu$m.

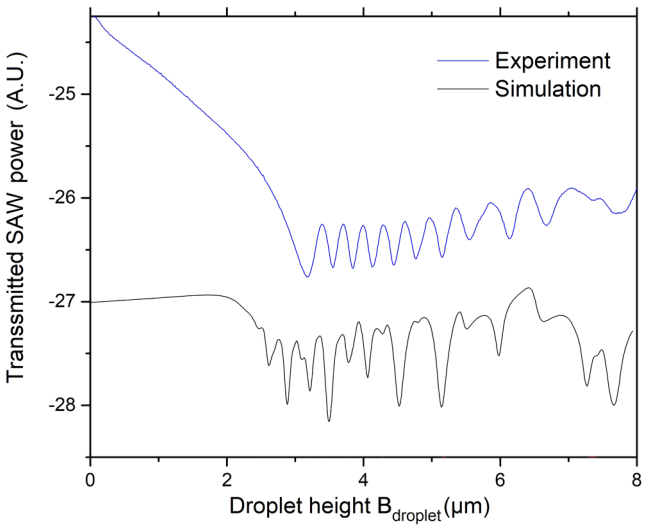

FIG. 13. Simulated transmitted SAW power of a 2D water droplet slice at $f_{SAW} = 160$ MHz and experimental transmitted SAW power at $f_{SAW} = 158$ MHz.

described by $h = R\tan(\theta/2)$, where R is the contact radius and θ is the contact angle, a small angle approximation can be applied to show the linearity. Alternatively, the height can be measured directly[23] or predicted by FEM simulation.[24] Knowing this linear time dependence of the height, the chirp in the height dependent signal must also exist in the time dependent one.

For a simple comparison of simulation and experiment, both the characteristic oscillations and the height of the drop were measured over time, allowing the oscillation frequency to be plotted as a function of the height as can be seen in Fig. 13, which shows very good agreement between the experimental and the simulated transmitted SAW power.

C. Summary of the two-dimensional analytical and simulational considerations and possible future approaches

The simulated and calculated transmission signals result from a 2D simplified model. This corresponds not to the real three-dimensional droplet shape. To get the whole picture, the droplet could, for example, be cut in various slices, where each slice is of a similar elliptic shape as in Fig. 10, but radius and height becoming smaller and smaller for the outer slices. After this step, a summation over the transmitted SAW power of every droplet slides would result in the corresponding three-dimensional signal. Furthermore, variations of the shrinking factor k and temperature behaviors due to the evaporation process are not yet considered. Another thing to note is that an elliptical droplet was used in the simulation for simplification purposes. But, unlike the real droplet, the elliptical droplet keeps its contact angle constant at 180° at any height. Still, with the chosen approaches, the main cause of the chirped oscillatory SAW transmission signal shortly before the complete evaporation has most likely been found.

V. CONCLUSION

In this study, the evaporation dynamics of small droplets on a solid substrate were investigated by employing SAW transmission experiments. We found characteristic oscillations in the SAW transmission shortly before complete evaporation of the droplets. Influences of various parameters on the properties of those oscillations were successfully investigated. We found that the oscillations can only be observed in the droplets with pinned contact lines and if the temperature is above the dew point. Their frequency is found to be proportional to the evaporation rate. Varying the SAW frequency showed a strong dependence on the oscillation frequency, which led to the explanation that vibrational modes are their cause. As the droplets shrinks, fewer modes can fit in and the conditions for constructive and destructive interference alternate, being reflected in the oscillations. Using different fluids reinforces the proportionality between the oscillations frequency and evaporation rate. Using water with various glycerol concentrations resulted in a decrease in the oscillations frequency at higher concentration. We strongly believe that our experimental findings together with the simulation based understanding of their origin might serve useful for the analysis of small complex fluid droplets as being used, for example, in DNA or protein based microarrays.

SUPPLEMENTARY MATERIAL

See the supplementary material for real-time measurement of the characteristic oscillations.

ACKNOWLEDGMENTS

We would like to acknowledge the Center for Nanoscience (CeNS), Nanosystems Initiative Munich (NIM), and Augsburg Centre for Innovative Technologies (ACIT) for their financial and technical support. Our sincere gratitude goes to Jürgen Neumann for drawing our attention to the dynamics of evaporating droplets, including the discussed physical phenomena, and Matthias Küß and Joshua Winkeljann for providing materials.

AUTHOR DECLARATIONS

Conflict of Interest

The authors have no conflicts to disclose.

DATA AVAILABILITY

The data that support the findings of this study are available within the article and its supplementary material.

REFERENCES

[1]R. D. Deegan, O. Bakajin, T. F. Dupont, G. Huber, S. R. Nagel, and T. A. Witten, Phys. Rev. E **62**, 756 (2000).
[2]C. H. Chon, S. Paik, J. B. Tipton, and K. D. Kihm, Langmuir **23**, 2953 (2007).
[3]B. Sobac and D. Brutin, Phys. Rev. E **86**, 021602 (2012).
[4]H. Gelderblom, A. G. Marín, H. Nair, A. van Houselt, L. Lefferts, J. H. Snoeijer, and D. Lohse, Phys. Rev. E **83**, 026306 (2011).
[5]Y. Kita, Y. Okauchi, Y. Fukatani, D. Orejon, M. Kohno, Y. Takata, and K. Sefiane, Phys. Chem. Chem. Phys. **20**, 19430 (2018).
[6]M. Birouk and S.C. Fabbro, Proc. Combust. Inst. **34**, 1577 (2013).

[7]K.-Y. Hashimoto and K.-Y. Hashimoto, *Surface Acoustic Wave Devices in Telecommunications* (Springer, 2000), Vol. 116.
[8]D. Morgan, *Surface Acoustic Wave Filters: With Applications to Electronic Communications and Signal Processing* (Academic Press, 2010).
[9]C. Campbell, *Surface Acoustic Wave Devices and Their Signal Processing Applications* (Elsevier, 2012).
[10]F. Josse, F. Bender, and R. W. Cernosek, Anal. Chem. **73**, 5937 (2001).
[11]X. Ding, P. Li, S.-C. S. Lin, Z. S. Stratton, N. Nama, F. Guo, D. Slotcavage, X. Mao, J. Shi, F. Costanzo *et al.*, Lab Chip **13**, 3626 (2013).
[12]T. Dung Luong and N. Trung Nguyen, Micro Nanosyst. **2**, 217 (2010).
[13]T. A. Franke and A. Wixforth, ChemPhysChem **9**, 2140 (2008).
[14]N. Lynn, C. Henry, and D. Dandy, Lab Chip **9**, 1780 (2009).
[15]Z. Guttenberg, H. Müller, H. Habermüller, A. Geisbauer, J. Pipper, J. Felbel, M. Kielpinski, J. Scriba, and A. Wixforth, Lab Chip **5**, 308 (2005).
[16]L. A. Legendre, J. M. Bienvenue, M. G. Roper, J. P. Ferrance, and J. P. Landers, Anal. Chem. **78**, 1444 (2006).
[17]V. Dugas, J. Broutin, and E. Souteyrand, Langmuir **21**, 9130 (2005).
[18]L. Rayleigh, Proc. London Math. Soc. **s1-17**, 4 (1885).
[19]R. J. Shilton, M. Travagliati, F. Beltram, and M. Cecchini, Adv. Mater. **26**, 4941 (2014).
[20]K. Gleason and S. A. Putnam, Langmuir **30**, 10548 (2014).
[21]T. W. G. van der Heijden, A. A. Darhuber, and P. van der Schoot, Langmuir **34**, 12471 (2018).
[22]I. G. Hwang, J. Y. Kim, and B. M. Weon, Appl. Phys. Lett. **110**, 031602 (2017).
[23]S. M. Rowan, M. I. Newton, and G. McHale, J. Phys. Chem. **99**, 13268 (1995).
[24]H. Hu and R. G. Larson, J. Phys. Chem. B **106**, 1334 (2002).